Journal of Southeast University (English Edition) Vol. 25, No. 1, pp. 47 – 51 Mar. 2009 ISSN 1003—7985

Prosthetic modeling for femoral head based on ellipsoid fitting

Liu Bin[1] Su Tieming[1] Ou Zongying[1] Zhao Dewei[2] Wang Weiming[2] Han Jun[3]

([1]Key Laboratory for Precision and Non-traditional Machining of Ministry of Education, Dalian University of Technology, Dalian 116024, China)
([2]Affiliated Zhongshan Hospital, Dalian University, Dalian 116001, China)
([3]Dalian Modern High-Tech Development Co., Ltd., Dalian 116025, China)

Abstract: A novel modeling method which can restore the shape of the femoral head with collapse induced by ischemic necrosis is proposed. First, sequential tomograms of the hip are obtained from a CT scan; secondly, an accurate and automatic method is used to extract the profile of the acetabulum; thirdly, a hybrid method is utilized to gather fiducial marks on the acetabulum; fourthly, bulky error sampling points are removed. Finally, an ellipsoid fitting method is used to fit the ellipsoid model of the femoral head. Two male sufferers with different necrosis extents are chosen as experimental subjects for contrastive simulation. Fifty cases of different ages (from 25 to 79 years old) are utilized for statistical comparisons of matching errors. The prosthetic models highly resemble the primary shape of the femoral head in health. This new method provides not only a theoretical model for accurate operation position fixing in an orthopaedics clinic, but it is also an innovative practical means for the individual manufacture of artificial femoral heads.

Key words: femoral head; ellipsoid; elimination; fitting; modeling

Avascular necrosis of the femoral head (ANFH) is a cosmopolitan disease. Reportedly, there are hundreds of thousands of new cases annually all over the world. At present, most scholars consider that if conservative treatment to ANFH is invalid, the best choice is most often the total hip joint replacements[1–3]. There are many varieties of artificial femoral head prostheses whether domestically made or imported. They are all manufactured under a uniform production and supply mode. But in fact, there are generally distinct differences in hip joint shapes between different persons. Therefore, the implanted femoral head prosthesis cannot always match the acetabulum well, and the sufferer's thighbone cannot move freely. So it becomes a current research focus in femoral head prosthetic treatment that reduces a necrotic femoral head to a former femoral head model in health. According to the existing literature, research on femoral head prosthetic modeling is still in its infancy. Kim et al. put forward that models of depressed femoral heads can be estimated by overlapping outlines of femoral heads[4]. Bassounas et al. assessed the dent extent of a necrotic femoral head using a volumetric method based on magnetic resonance imaging data[5]. Although the results accelerated the development of femoral head prosthesis research, they mostly used probability statistical results from multi-case samples to describe a femoral head's state after necrosis, and they could not reconstruct the defective femoral head's shape. Another serious shortcoming was to suppose the femoral head to be a sphere, which brought a tremendous error to the factual parameter. The existing researches have proved that the femoral head's shape is not a sphere but an ellipsoid[6].

A new method for the recuperating model of a necrotic femoral head is presented. Briefly stated, a femoral head is regarded as an ellipsoid. Then, the femoral head's configuration is reverted by data points on an unspoiled acetabulum. Adopting this method, the bone surgery of the Affiliated Zhongshan Hospital of Dalian University actualized prosthetic simulation for the necrotic femoral head preoperatively. Proved by clinical feedback, doctors can preoperatively ascertain the boundary dimensions of the target femoral head with accuracy. This innovative means can shorten surgery time to a large extent, and further improve surgery quality.

1 Structure of Hip Joint and Prosthetic Purpose

The hip joint is composed of a femoral head and an acetabulum. As shown in Fig. 1, there is a semilunar articular facet in the acetabulum, which is called the lunate surface. The acetabular fossa is a hollow in the acetabulum, and it does not form into an articular facet. The indentation below the limbus of the acetabulum is called the acetabular notch. The femoral head is located on the superior extremity of the thighbone, which is the longest bone in body. The femoral head joints with the lunate surface. The articular facet of the femoral head is about two-thirds of an approximative spherical surface, which is almost all enveloped by the acetabulum. The femoral head and the acetabulum are spherically jointed by the contact surface of the lunate surface.

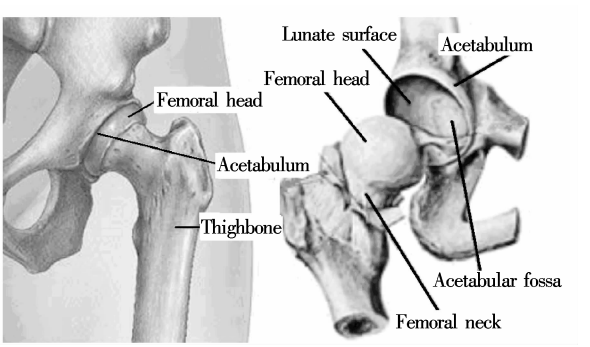

Fig. 1 Structure of hip joint

The essential symptom for avascular necrosis of the femoral head is cystoid subsiding on the spherical surface of the femoral head, which induces suffocation of the slip connec-

Received 2008-08-20.
Biographies: Liu Bin (1981—), male, graduate; Ou Zongying (corresponding author), male, professor, ouzyg@dlut.edu.cn.
Foundation items: The National High Technology Research and Development Program of China (863 Program) (No. 863-306-ZD13-03-6), the High Technology Research and Development Program of Dalian City (No. 2005E21SF134).
Citation: Liu Bin, Su Tieming, Ou Zongying, et al. Prosthetic modeling for femoral head based on ellipsoid fitting[J]. Journal of Southeast University (English Edition), 2009, 25(1): 47 – 51.

tion between the femoral head and the acetabulum. Consequently, the prosthetic purpose is to renew the necrotic femoral head to become the spherical model in health, and accordingly resumes the normal spherically jointed movement between the femoral head and the acetabulum.

2 Edge Extracting of Acetabulum

After collecting the sequential faulting images of the femoral head utilizing a multi-slice helical CT, an accurate and automatic segmentation method is used to extract the edge of the acetabulum[7], and to synchronously remove other tissues in the images (see Fig. 2). The processing scheme consists of the following five steps: 1) Preprocessing, including resampling 3D CT data by a modified Sinc interpolation to create isotropic volume and to avoid Gibbs ringing, and smoothing the resulting images by a 3D Gaussian filter; 2) Detecting bone tissues from CT images by conventional techniques, including histogram-based thresholding and binary morphological operations; 3) Estimating the initial boundaries of the femoral head and the joint space between the acetabulum and the femoral head by a new approach of utilizing the constraints of the greater trochanter and the shapes of the femoral head; 4) Enhancing the joint space by a Hessian filter; and 5) Refining the rough boundaries obtained in step 3) by a moving disk technique and the filtered images obtained in step 4).

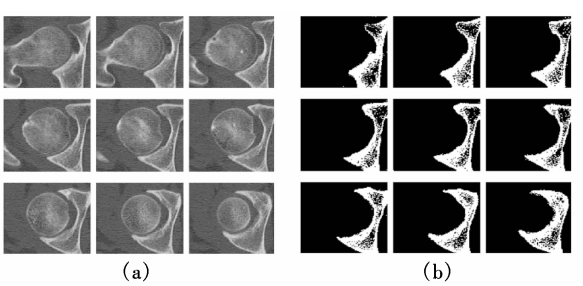

Fig. 2 Edge extracting from CT images. (a) Original images; (b) Binary images of the acetabulum

3 Sampling of Data Points

After obtaining binary images for the figure of the acetabulum, the next process is to collect data points of the lunate surface in each layer image. A familiar sampling method is equidistant raster sampling, which samples via the intersecting of raster and the target figure. While sampling for the acetabulum using the method, worthless points outside the lunate surface will also be collected and the collected points on the acetabulum are distributed unequally. There are only a few sampling points on the lunate surface, which tightly contact with the femoral head. Therefore, according to the special construction feature, a hybrid method based on equidistant raster sampling and spoke wire sampling[8] is presented for making the sampling process more equal and rational. The steps are listed as follows:

1) Collecting some sampling points on the lunate surface utilizing equidistant raster (12 sampling points in this paper, as shown in Fig. 3(a)).

2) Taking N triplets of points in the sampling point set. Each triplet is composed of three random non-collinear coordinate points $C_k(x_k, y_k)$, $k = 1, 2, 3$.

3) Substituting $C_k(x_k, y_k)$ into the general equation of the circle $x^2 + y^2 + D_x + E_y + F = 0$.

Solving a definite value $(X_c, Y_c) = (-D_x/2, -E_y/2)$ for the center of this circle by these three points. Here

$$E_y = \frac{(x_1 - x_2)N - (x_2 - x_3)M}{(y_1 - y_2)(x_2 - x_3) - (y_2 - y_3)(x_1 - x_2)}$$

$$D_x = \frac{-M - (y_1 - y_2)E_y}{x_1 - x_2}$$

where $M = x_1^2 + y_1^2 - x_2^2 - y_2^2$; $N = x_2^2 + y_2^2 - x_3^2 - y_3^2$.

4) Computing the fiducial value of the center coordinate:

$$X_b = \frac{1}{N}\sum_{t=1}^{N} X_{ct}, \quad Y_b = \frac{1}{N}\sum_{t=1}^{N} Y_{ct}$$

5) Projecting spoke wires around with a certain value of the included angle between two adjacent wires (10° in this paper). When a wire intersects with the figure of the acetabulum, a coordinate sampling point is obtained, as shown in Fig. 3(b).

At the same computation cost, 17 sampling points are collected through the equidistant raster sampling method with five useless points (as shown in Fig. 3(c)) and a sample qualification rate of 70.59%. Yet all the 17 sampling points collected through the hybrid method are valid points with a rational distribution.

6) Centralizing the coordinate system in order to avoid numerical calculation problems caused by large numerical values:

$$\{x_i'', y_i'', z_i''\}^T = \{x_i', y_i', z_i'\}^T - \{\overline{x'}, \overline{y'}, \overline{z'}\}^T$$

where $\overline{x'}, \overline{y'}, \overline{z'}$ are the means of coordinate components.

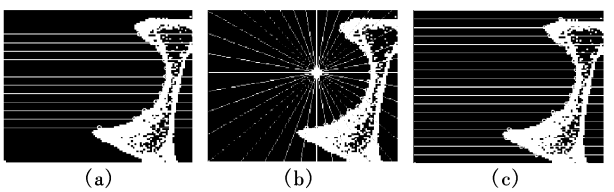

Fig. 3 Sampling of point set. (a) Preliminary sampling; (b) Spoke wire sampling; (c) Contrastive sampling

4 Elimination of Error Sampling Points

The concave surface, on which the lunate surface is located, can be fitted utilizing the space coordinate sampling point set that has been collected in the sequential images. However, not all the coordinates in the point set are accurate data. There are two inducements importing errors: 1) Some sampling points containing large error amounts are imported when the sampling wires detect these non-articular facets, as shown in Fig. 4(a); 2) Some sampling points can be incorporated with errors of coordinates due to measuring accuracy.

Since the concave surface that the lunate surface is located on is an approximate sphere, it is assumed to be a sphere S_A. S_F is a convex surface that the femoral head locates on. Because the relative motion between the femoral head and the acetabulum is spherically articulated, S_A and S_F are concentric spheres. It can be considered that the radius of S_F and

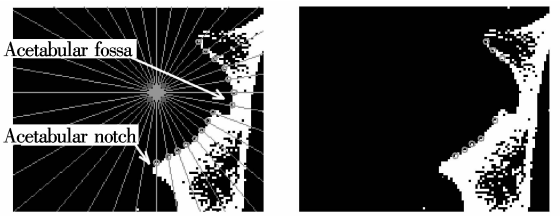

Fig. 4 Elimination of error sampling points. (a) Before eliminating; (b) After eliminating

S_A are also equal. Suppose that the surface equation of S_A is

$$(x - X)^2 + (y - Y)^2 + (z - Z)^2 = R^2 \tag{1}$$

Then the elimination process is as follows:

1) Taking N quadruples of points in the sampling point set. Each quadruple is composed of four random non-coplanar coordinate points $P_k(x_k, y_k, z_k)$, $k = 1, 2, 3, 4$.

2) Substituting $P_k(x_k, y_k, z_k)$ into surface Eq. (1). A definite value for the center and radius of this sphere can be solved by these four points:

$$X_c = \frac{\boldsymbol{H}}{\boldsymbol{G}}, \quad Y_c = \frac{\boldsymbol{I}}{\boldsymbol{G}}, \quad Z_c = \frac{\boldsymbol{J}}{\boldsymbol{G}}$$

$$R_c = \sqrt{(x_k - X_c)^2 + (y_k - Y_c)^2 + (z_k - Z_c)^2}$$

where

$$\boldsymbol{H} = \begin{vmatrix} s_2 & y_2 - y_1 & z_2 - z_1 \\ s_3 & y_3 - y_1 & z_3 - z_1 \\ s_4 & y_4 - y_1 & z_4 - z_1 \end{vmatrix}, \quad \boldsymbol{I} = \begin{vmatrix} x_2 - x_1 & s_2 & z_2 - z_1 \\ x_3 - x_1 & s_3 & z_3 - z_1 \\ x_4 - x_1 & s_4 & z_4 - z_1 \end{vmatrix}$$

$$\boldsymbol{J} = \begin{vmatrix} x_2 - x_1 & y_2 - y_1 & s_2 \\ x_3 - x_1 & y_3 - y_1 & s_3 \\ x_4 - x_1 & y_4 - y_1 & s_4 \end{vmatrix}, \quad \boldsymbol{G} = \begin{vmatrix} x_2 - x_1 & y_2 - y_1 & z_2 - z_1 \\ x_3 - x_1 & y_3 - y_1 & z_3 - z_1 \\ x_4 - x_1 & y_4 - y_1 & z_4 - z_1 \end{vmatrix}$$

$$s_j = \frac{x_j^2 + y_j^2 + z_j^2 - x_1^2 - y_1^2 - z_1^2}{2} \qquad j = 2, 3, 4$$

3) Computing the fiducial value of the center coordinate:

$$X_b = \frac{1}{N}\sum_{t=1}^{N} X_{ct}, \quad Y_b = \frac{1}{N}\sum_{t=1}^{N} Y_{ct}$$

$$Z_b = \frac{1}{N}\sum_{t=1}^{N} Z_{ct}, \quad R_b = \frac{1}{N}\sum_{t=1}^{N} R_{ct}$$

4) Calculating the residual error of each sampling point by traversing the coordinates sampling point set:

$$v_i = \sqrt{(x_i - X_b)^2 + (y_i - Y_b)^2 + (z_i - Z_b)^2} - R_b$$

The Laiyite criterion (3σ) is adopted to eliminate error sampling points. The constraints of the universal distribution range are also required; namely, sampling points must be equably distributed over a wide range.

5) Computing the standard deviation estimator s according to the Bessel formula:

$$s = \sqrt{\frac{\sum_{i=1}^{n} v_i^2}{n - 1}}$$

If some sampling point (x_l, y_l, z_l) satisfies $|v_l| > 3s$, it can be regarded as a gross error point. Besides, if there are valid sampling points in the scope of two adjacent spoke wires to this sampling point's spoke wire, eliminate this sampling point (x_l, y_l, z_l).

6) Updating the space coordinate sampling point set and repeating steps 1) to 5) circularly. When there is no gross error sampling point, end elimination. The sampling points after eliminating errors are shown as some small circles in Fig. 4(b).

5 Fitting of Femoral Head Ellipsoid

After obtaining the space coordinate sampling point set composed of normal data, the ellipsoid, which the femoral head is located on, can be accurately fitted utilizing these points. The ellipsoid fitting method in this paper starts from a general equation of the quadratic surface:

$$F(\boldsymbol{a}, \boldsymbol{x}) = a_1x^2 + a_2xy + a_3y^2 + a_4xz + a_5yz + a_6z^2 + a_7x + a_8y + a_9z + a_{10} = \boldsymbol{a}^T \cdot \boldsymbol{x} = 0 \tag{2}$$

where $\boldsymbol{a} = \{a_1, a_2, \ldots, a_{10}\}^T$, $\boldsymbol{x} = \{x^2, xy, y^2, xz, yz, z^2, x, y, z, 1\}^T$.

Eq. (2) can be rewritten in the form of

$$F(\boldsymbol{A}, \boldsymbol{b}, c, \boldsymbol{x}) = \boldsymbol{x}^T\boldsymbol{A}\boldsymbol{x} + \boldsymbol{b}^T\boldsymbol{x} + c = 0 \tag{3}$$

where

$$\boldsymbol{A} = \begin{bmatrix} a_1 & \frac{a_2}{2} & \frac{a_4}{2} \\ \frac{a_2}{2} & a_3 & \frac{a_5}{2} \\ \frac{a_4}{2} & \frac{a_5}{2} & a_6 \end{bmatrix} = \begin{bmatrix} \boldsymbol{U} & \boldsymbol{v} \\ \boldsymbol{v}^T & a_6 \end{bmatrix}$$

$$\boldsymbol{b} = \begin{Bmatrix} a_7 \\ a_8 \\ a_9 \end{Bmatrix}, \quad c = a_{10}$$

$$\boldsymbol{U} = \begin{bmatrix} a_1 & \frac{a_2}{2} \\ \frac{a_2}{2} & a_3 \end{bmatrix}, \quad \boldsymbol{v} = \begin{Bmatrix} \frac{a_4}{2} \\ \frac{a_5}{2} \end{Bmatrix}$$

An effective and efficient ellipsoid fitting algorithm is adopted, which will not lead to nonlinear optimization. When the leading form is positive definite, the solutions of a quadratic equation must be bounded and restrict the model to be an ellipsoid. Lemma 1 provides constraints forcing a general 3D quadric surface to be an ellipsoid[9].

Lemma 1 $\boldsymbol{A}$ is positive definite or negative definite iff

$$\det(\boldsymbol{U}) > 0 \Leftrightarrow 4a_1a_3 - a_2^2 > 0, \quad (a_1 + a_3)\det(\boldsymbol{A}) > 0$$

The problem of fitting an ellipsoid into N data points $\boldsymbol{x}_i$ can be solved by minimizing the sum of squares of the "algebraic distances"

$$E = \sum_{i=1}^{N} F^2(\boldsymbol{a}, \boldsymbol{x}_i) = \| \boldsymbol{D}\boldsymbol{a} \|^2 \tag{4}$$

where $\boldsymbol{D} = [\boldsymbol{x}_1 \quad \boldsymbol{x}_2 \quad \ldots \quad \boldsymbol{x}_N]^T$. $\boldsymbol{a}$ is subject to the constraint $\boldsymbol{a}^T\boldsymbol{C}\boldsymbol{a} = 1$. Since a_1 is a free parameter, the first condition of

lemma 1 can be converted into an equality, as in the case for 2-D fitting. Thus, the constraint can be written as $\boldsymbol{a}^{\mathrm{T}}\boldsymbol{C}\boldsymbol{a}=1$, where

$$\boldsymbol{C}_{10\times10}=\begin{bmatrix}0&0&2&0&\cdots&0\\0&-1&0&0&\cdots&0\\2&0&0&0&\cdots&0\\0&0&0&0&\cdots&0\\\vdots&\vdots&\vdots&\vdots&&\vdots\\0&0&0&0&\cdots&0\end{bmatrix} \tag{5}$$

The minimization problem brought by Eqs. (4) and (5) can be solved by a Lagrange multiplier. Hence, the solution $\boldsymbol{a}$ is the generalized eigenvector of

$$\boldsymbol{D}^{\mathrm{T}}\boldsymbol{D}\boldsymbol{a}=\lambda\boldsymbol{C}\boldsymbol{a} \tag{6}$$

corresponding to the smallest positive eigenvalue. It is easy to verify that the quadric surface is an ellipsoid by validating that the second condition of lemma 1 is satisfied.

6 Experimental Results and Analysis

CT images of two sufferers are used as experimental data for prosthetic simulation: case 1, 28-year-old, male, first phase necrosis condition; case 2, 59-year-old, male, third phase necrosis condition. On the basis of the existent medical image processing and the 3D reconstruction system[10], a special functional module is developed for prosthetic modeling of the femoral head. Results after prosthesis are shown in Fig. 5. For each case, by comparing the pictures in the first row with the pictures in the second row and comparing the unrepaired model with the repaired model, it can be seen that necrotic femoral heads are all reduced to their healthy models.

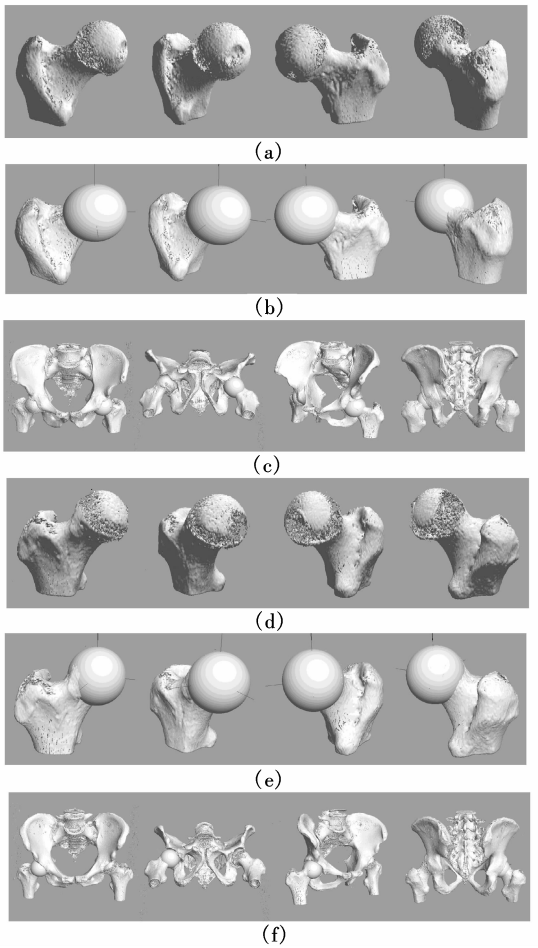

Fig. 5 Prosthetic modeling of femoral head for case 1 and case 2. (a) Left-hand morbid femoral head 3D reconstruction of case 1; (b) Left-hand prosthetic femoral head 3D reconstruction of case 1; (c) Total hip 3D reconstruction of case 1; (d) Right-hand morbid femoral head 3D reconstruction of case 2; (e) Right-hand prosthetic femoral head 3D reconstruction of case 2; (f) Total hip 3D reconstruction of case 2

Since different experimental subjects have different data complexities, the computation costs are also different. For a same subject(case 1, 16 bit × 512 row × 512 column × 100 slice), compared with Kim's fitting method of stacking multi-contour, the amount of calculation for the suggested method is reduced by 26%. And for importing the optimized mechanism of elimination, the precision of the prosthetic model is obviously improved. Compared with Bassounas' volume rendering method, data throughput for the suggested method is reduced by 66%. In addition, these two methods need multi-case samples to be statistically analyzed, and they can only reflect a morbid femoral head state. The suggested method only processes image data of a target case, and can reconstruct a model in health.

Compared with the method presented in Ref. [8], a statistical analysis of matching accuracy between the acetabulum and the reconstructed model is implemented. In Ref. [8], a femoral head was fitted to be a sphere, which led to large errors in the factual parameters. Image data of fifty cases of different ages (from 25 to 79 years old) are utilized as experimental subjects. The method in Ref. [8] and the suggested method were synchronously practiced on the same case. In Fig. 6, the fitted spheres are displayed in the surface form, and the fitted ellipsoids are displayed in the point form. The statistical parameter is the matching error; namely, the average distance between sampling points on the acetabulum and the sphere or the ellipsoid. Three characteristics

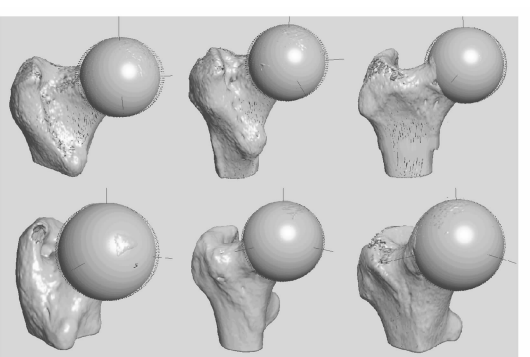

Fig. 6 Comparison of ellipsoid fitting and sphere fitting

can be deduced from Fig. 7: 1) The matching error of the sphere fitting method is on a downtrend with increasing age; 2) The matching error of the ellipsoid fitting method is almost unchanged with increasing age; 3) The matching errors of these two methods are gradually approximate with increasing age. From 3), it can be deduced that the femoral heads of young sufferers show significant differences to the sphere model and this difference becomes smaller with increasing age. Moreover, the femoral heads of old sufferers tend to be spheres.

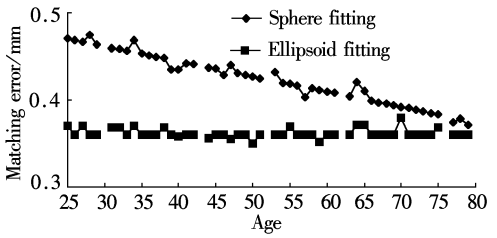

Fig. 7 Statistic analysis of matching accuracy

7 Conclusion

A new method which can restore necrotic femoral heads into original models in health is presented. An accurate automatic segmentation method is used to extract acetabulum contours. A hybrid sampling method is utilized to collect equal and rational points, and error data are eliminated. The ellipsoid model is constructed by a general equation of the quadratic surface. Experiments show that this method can well reconstruct the femoral head model in health of a target case. It has obtained good results when used in clinical practice. Comparing with other methods, it has the advantages of fast calculation and high precision. Meanwhile, it can be concluded that the femoral heads of young sufferers differ significantly from the sphere model and this difference becomes smaller with increasing age. Also, the femoral heads of old sufferers tend to be spheres.

References

[1] Sharma N, Meyer D. Design of a dimpled femoral head in total hip replacements using elastohydrodynamic lubrication theory[C]//*Proceedings of the IEEE* 31*st Annual Northeast on Bioengineering*. Hoboken, NJ, USA, 2005: 92 - 93.

[2] Zhao Dewei, Wang Weiming, Wang Benjie, et al. Conservative methods for osteonecrosis of the femoral head: the review of 1005 cases[J]. *Chinese Journal of Surgery*, 2005, **43**(16): 1054 - 1057. (in Chinese)

[3] Sarry L, Tilmant C, Boisgard S, et al. Monitoring of polyethylene wear in nonmetal-backed acetubular cups by digitized anteroposterior pelvic radiography[J]. *IEEE Transactions on Medical Imaging*, 2003, **22**(9): 1172 - 1182.

[4] Kim J S, Kim S I. A new measurement method of femoral anteversion based on the 3D modeling[C]//*Proceedings of the* 19*th Annual International Conference of the IEEE on Engineering in Medicine and Biology Society*. Chicago, USA, 1997, **1**: 418 - 421.

[5] Bassounas A, Fotiadis D I, Malizos K N. Evaluation of femoral head necrosis using a volumetric method based on MRI [C]//*Proceedings of the* 23*rd Annual International Conference of the IEEE on Engineering in Medicine and Biology Society*. Istanbul, Turkey, 2001, **2**: 1532 - 1535.

[6] Baruffaldi F, Bettuzzi M, Bianconi D, et al. An innovative CCD-based high-resolution CT system for analysis of trabecular bone tissue[J]. *IEEE Transactions on Nuclear Science*, 2006, **53**(5): 2584 - 2590.

[7] Zoroofi R A, Sato Y, Sasama T, et al. Automated segmentation of acetabulum and femoral head from 3-D CT images [J]. *IEEE Transactions on Information Technology in Biomedicine*, 2003, **7**(4): 329 - 343.

[8] Liu Bin, Song Weiwei, Ou Zongying, et al. Reparative modeling for femoral head based on eliminative fitting[J]. *Journal of Southeast University*: *Natural Science Edition*, 2008, **38**(1): 58 - 63. (in Chinese)

[9] Fitzgibbon A W, Pilu M, Fisher R B. Direct least-square fitting of ellipses[J]. *IEEE Transactions on Pattern Analysis and Machine Intelligence*, 1999, **21**(5): 476 - 480.

[10] Ou Zongying, Qin Xujia, Ji Fengxin, et al. Study and development of image & graphics processing software of multi-leaf collimator conformal radiotherapy system [J]. *Journal of Dalian University of Technology*, 2001, **41**(6): 711 - 715. (in Chinese)

基于椭球面拟合的股骨头修复建模

刘 斌[1] 苏铁明[1] 欧宗瑛[1] 赵德伟[2] 王卫明[2] 韩 军[3]

([1] 大连理工大学精密与特种加工教育部重点实验室,大连 116024)

([2] 大连大学附属中山医院,大连 116001)

([3] 大连现代高技术发展有限公司,大连 116025)

摘要:提出了一种可以获得目标病例健康时股骨头模型的新建模方法. 首先利用一种精确的自动分割方法在髋骨部位 CT 序列图像中提取髋臼轮廓;然后使用基于等距栅格采样法与辐条式采样法相结合的混合采样法得到髋臼凹面的空间坐标点集,并剔除其中的误差采样点;最后采用基于二次曲面一般方程的方法拟合原始股骨头椭球面模型. 通过对 2 例不同坏死程度的男性患者进行修复性的对比仿真,以及对 50 例不同年龄(25 ~ 79 岁)患者修复重建后的匹配误差统计分析,证明此方法可以良好地还原坏死的股骨头模型,既为骨科临床中的精确手术定位提供了理论模型,又为针对个体化制造的人工假体生产提供了新的实践方法.

关键词:股骨头;椭球面;剔除;拟合;建模

中图分类号:TP391